Heliyon

In silico study of 4-phosphorylated derivatives of 1,3-oxazole as inhibitors of *Candida albicans* fructose-1,6-bisphosphate aldolase II

Ivan V. Semenyuta [a],[*]**, Oleksandr L. Kobzar** [b]**, Diana M. Hodyna** [a]**,**
Volodymyr S. Brovarets [c]**, Larysa O. Metelytsia** [a]

[a] *Department of Medical and Biological Researches, V.P. Kukhar Institute of Bioorganic Chemistry and Petrochemistry of the National Academy of Sciences of Ukraine, Kyiv, Ukraine*

[b] *Department of Bioorganic Mechanisms, V.P. Kukhar Institute of Bioorganic Chemistry and Petrochemistry of the National Academy of Sciences of Ukraine, Kyiv, Ukraine*

[c] *Department of Chemistry of Bioactive Nitrogen Containing Heterocyclic Bases, V.P. Kukhar Institute of Bioorganic Chemistry and Petrochemistry of the National Academy of Sciences of Ukraine, Kyiv, Ukraine*

[*] Corresponding author.

E-mail address: ivan@bpci.kiev.ua (I.V. Semenyuta).

Abstract

In this study, the synthesis, *in vitro* anti-Candida activity and molecular modeling of 4-phosphorylated derivatives of 1,3-oxazole as inhibitors of *Candida albicans* fructose-1,6-bisphosphate aldolase (FBA-II) are demonstrated and discussed. Significant similarity of the primary and secondary structure, binding sites and active sites of FBA-II *C. albicans* and *Mycobacterium tuberculosis* are established. FBA-II *C. albicans* inhibitors contained 1,3-oxazole-4-phosphonates moiety are created by analogy to inhibitors FBA-II *M. tuberculosis*. The experimental studies of the anti-Candida activity of the designed and synthesized compounds have shown their high activity against standard strain and its *C. albicans* fluconazole resistant clinical isolate. It was hypothesized that the growth suppression of fluconazole-resistant C. *albicans* strain may be due to the inhibition of aldolase fructose-1,6-bisphosphate. A qualitative homology 3D

model of the *C. albicans* FBA-II was created using SWISS-MODEL server. The probable mechanism of FBA-II inhibition by studied 4-phosphorylated derivatives was shown using molecular docking. The main role of amino acid residues His110, His226, Gly227, Leu248, Val238, Asp144, Lys230, Glu147, Gly227, Ala112, Leu145 and catalytic zinc atom in the formation of stable ligand-protein complexes with $\Delta G = -6.89, -7.2, -7.16, -7.5, -8.0, -7.9$ kcal/mol was shown.

Thus, the positive results obtained in the work were demonstrated the promise of using the proposed homology 3D model of the *C. albicans* FBA-II as the target for the search and development of new anti-Candida agents against azole-resistant fungal pathogens. Designed and studied 4-phosphorylated derivatives of 1,3-oxazole having a direct inhibiting FBA-II molecular mechanism of action can be used as perspective drug-candidates against resistant *C. albicans* strains.

Keywords: Microbiology, Pharmaceutical science, Organic chemistry

1. Introduction

Fungal infections are the important problems of modern world healthcare system. Candidiasis is the main systemic human infection. *Candida* spp. is an opportunistic pathogen causing serious pathology in patients with impaired immunity. *Candida* spp. can lead to severe systemic infections and to mortality in patients with various types immunodeficiency [1, 2].

Modern anti-Candida drugs include such antifungal agents as azoles, echinocandins, polyenes and flucytosine (5-FC) [3]. Echinocandins inhibit the synthesis of β-glucan [4]. Polyenes (amphotericin B) act by creating of the complexes with ergosterol of the plasma membrane [5]. Flucytosine blocks the DNA synthesis, leading to the disruption to DNA replication [6]. Azoles are the most numerous antifungal agents known since the 1960s [7]. Azoles are completely synthetic compounds, classified as imidazoles and triazoles and are the rapidly developing group of antifungal compounds. The sterol 14α-demethylase (CYP51) is the azoles target in which the five-membered azole ring forms a coordination bond with iron heme by inhibiting the ergosterol biosynthesis. Rapid formation of *Candida* spp. multidrug resistance is the ground for the drugs development with new alternative targets. In our opinion, fructose-1,6-bisphosphate aldolase is a promising target for the development of new antifungal agents.

Its known, fructose-1,6-bisphosphate aldolase (FBA-II, EC4.1.2.13) is an important enzyme of glycolysis, gluconeogenesis and the Calvin cycle. This class II enzyme is a zinc-containing protein that catalyzes the reversible cleavage of fructose-1,6-bisphosphate (FBP) to dihydroxyacetone phosphate (DHAP) and glyceraldehyde-

3-phosphate (GAP) [8]. The FBA-II uses a bivalent zinc ion to polarize and stabilize the ketocarbonyl group of the substrate and its intermediate enediolate. FBA-II is present in pathogenic microbes - fungi, bacteria and parasites but is absent in higher plants and mammals that make it a convenient selective target for the development of new antifungal agents [9]. The studies of this enzyme inhibitors for various organisms, including *M. tuberculosis* [10], *Bacillus subtilis* [11], *Pseudomonas aeruginosa* [12] and *Streptococcus pneumoniae* [13] are known. Rodaki A. et al. [9] studied the depletion effect of *C. albicans* FBA-II as an antifungal drugs target. These results showed that an enzyme level decrease to less than 5% causes the *C. albicans* growth inhibition. A number of substrate-like FBA-II inhibitors have been developed, however, they did not provide an adequate level of structural specificity required for effective drug-candidates [9].

In our work we represent the *in silico* study, synthesis and antifungal evaluation of series 4-phosphorylated derivatives of 1,3-oxazoles with antifungal special mechanism of action as perspective candidates of new antifungal agents against *C. albicans*.

2. Materials and methods

2.1. Chemistry

The IR spectra of substances were registered (KBr disks) by using Bruker VERTEX 70 FT-IR spectrometer (Bruker, Rheinstetten, Germany). ^{1}H NMR and ^{31}P NMR spectroscopy of compouds in DMCO-d$_6$ solution were coursed by Bruker AVANCE DRX-500 4-channel spectrometer. NMR chemical shifts are given with tetramethyl-silane as internal standard for NMR spectra ^{1}H and with phosphoric acid (85%) as external standard for NMR spectra [31]P. Melting points were measured by a Fisher-Johns melting point apparatus (Fisher Scientific Co., St. Louis, USA) and are uncorrected. The reaction course and the purity of the synthesized compounds were monitored by Merck silica gel 60 F254 plates, also elemental analyses were carried out in analytical laboratories.

Synthesis of *1-[4-(diethoxyphosphoryl)-2-methyl-1,3-oxazol-5-yl]piperidin-4-ylcarboxylic acid* **1**, and also acids, needed for syntheses of appropriate sodium salts **2** and **3** is shown on Scheme 1 [14].

Sodium salt of 1-[4-(diethoxyphosphoryl)-4-methylphenyl-1,3-oxazol-5-yl]piperidin-4-ylcarboxylic acid **2** was prepared by evaporation to dryness under a reduced pressure of mixture aqueous solution of 1 mmol 1-[4-(diethoxyphosphoryl)-4-methylphenyl-1,3-oxazol-5-yl]piperidin-4-ylcarboxylic acid and 1 mmol of sodium bicarbonate which used without further purification for biological tests.
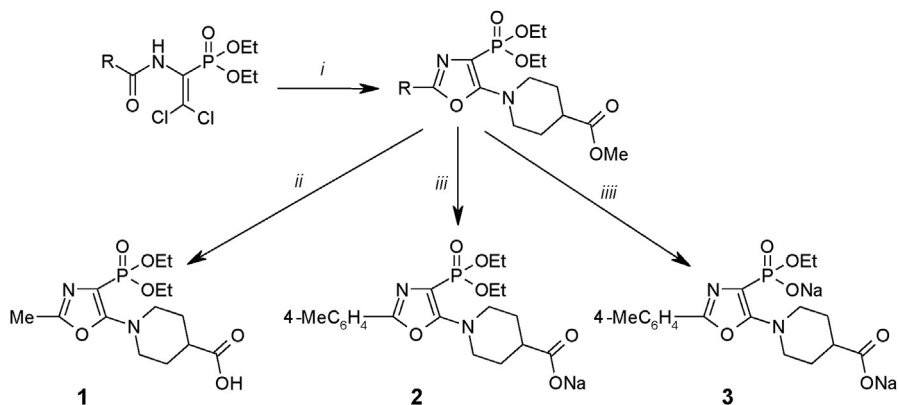
Scheme 1. Reagents and conditions: (*i*) methyl isonipecotinate/Et$_3$N(exc.)/MeOH, 3h, reflux. (*ii*) R = Me; 1eq NaOH/H$_2$O, 30h, RT. (*iii*) R = 4-MeC$_6$H$_4$; 1. 1eq NaOH/H$_2$O, 30h, RT; 2. 1eq NaHCO$_3$/H$_2$O, RT. (*iiii*) R = 4-MeC$_6$H$_4$; 1. 4eq NaOH/EtOH, 10 days, RT; 2. 2eq NaHCO$_3$/H$_2$O, RT.

Disodium salt of 1-[4-hydroxy(ethoxy)phosphoryl-(4-methylphenyl)-1,3-oxazol-5-yl]piperidin-4-carboxylic acid **3** was prepared by evaporation to dryness under a reduced pressure of mixture aqueous solution of 1 mmol 1-[4-hydroxy(ethoxy)phosphoryl-(4-methylphenyl)-1,3-oxazol-5-yl]piperidin-4-carboxylic acid and 2 mmol of sodium bicarbonate which used without further purification for biological tests.

Synthesis of sodium salts **4**−**6** has been previously reported [15]. Their precursors − diethyl 5-arylsulfanyl-2-(4-methylphenyl)-1,3-oxazol-4-ylphenylphosphonates − were prepared according to the previously described method (Scheme 2).

Disodium salt of 5-(4-chlorophenylsulfanyl)-2-(4-methylphenyl)-1,3-oxazol-4-ylphosphonic acid **4** was prepared by evaporation to dryness under a reduced pressure of mixture aqueous solution of 1 mmol 5-(4-chlorophenylsulfanyl)-2-(4-methylphenyl)-1,3-oxazol-4-ylphosphonic acid and 2 mmol of sodium bicarbonate which used without further purification for biological tests.
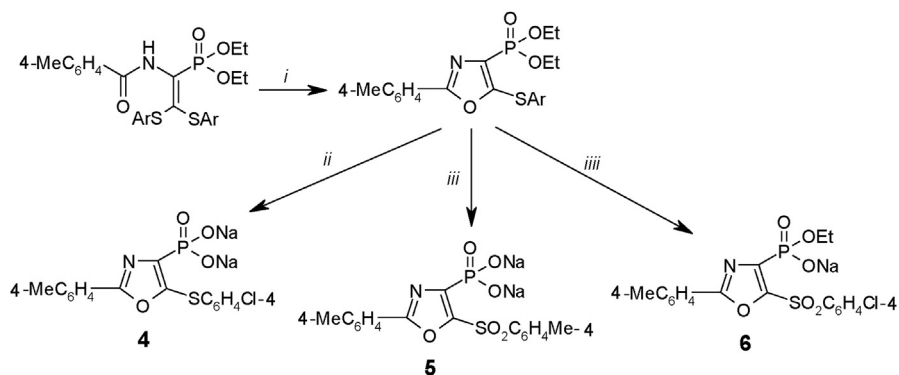
Scheme 2. Reagents and conditions: (*i*) Ag$_2$CO$_3$(exc.)/dioxan, 8h, reflux; (*ii*) Ar = 4-ClC$_6$H$_4$; 1. HBr/MeCOOH, 6h, RT; 2. 2eq NaHCO$_3$/H$_2$O, RT; (*iii*) Ar = 4-MeC$_6$H$_4$; 1. HBr/MeCOOH, 6h, RT; 2. H$_2$O$_2$/MeCOOH, 2h, reflux; 3. 2eq NaHCO$_3$/H$_2$O, RT; (*iiii*) Ar = 4-ClC$_6$H$_4$; 1. HBr/MeCOOH, 6h, RT; 2. H$_2$O$_2$/MeCOOH, 2h, reflux; 3. 1eq NaHCO$_3$/H$_2$O, RT.

Disodium salt of 2-(4-methylphenyl)-5-(4-methylphenylsulfonyl)-1,3-oxazol-4-ylphosfonyl acid **5.** 2-(4-Methylphenyl)-5-(4-methylphenylsulfanyl)-1,3-oxazol-4-ylphosfanyl acid (10 mmol) was dissolved in 15 ml of anhydrous acetic acid, heated to 90−100 °C, and hydrogen peroxide 35% aqueous solution (36 mmol) was added dropwise, the mixture refluxed for 2 hours, evaporated *in vacuo* to dryness, the residue was triturated with water, precipitate filtered, recrystallized from ethanol. The yield of *2-(4-methylphenyl)-5-(4-methylphenylsulfonyl)-1,3-oxazol*-4-yl *phosphonic acid* was 83%. M.p. 246−248 °C. IR (KBr): ν cm^{-1}: 1344 (SO$_2$), 1177 (SO$_2$), 1227 (P=O). ^{1}H NMR (DMSO-d$_6$): δ(ppm) 8.08, 7.86, 7.48, 7.38 (m, 8H, 2C$_6$H$_4$), 2.40 (s, 3H, CH$_3$), 2.38 (s, 3H, CH$_3$). ^{31}P NMR (DMSO-d$_6$), δ(ppm) -2.5. Anal. Calcd. for C$_{17}$H$_{16}$NO$_6$PS: N, 3.56; P, 7.78; S, 8.15; Found: N, 3.43; P, 7.91; S, 8.27. Disodium salt **5** was prepared by evaporation to dryness under a reduced pressure of mixture aqueous solution of 1 mmol of acid and 2 mmol of sodium bicarbonate which used without further purification for biological tests.

Sodium salt of monoethyl ester 5-(4-chlorophenylsulfonyl)-2-(4-methylphenyl)-1,3-oxazol-4-ylphosphonic acid **6** (10 mmol) was dissolved in 15 ml of anhydrous acetic acid, heated to 90−100 °C, and hydrogen peroxide 35% aqueous solution (36mmol) was added dropwise, the mixture refluxed for 2 hours, evaporated *in vacuo* to dryness, the residue was triturated with water, precipitate filtered, recrystallized from ethanol. The yield of *monoethyl ester 2-(4-methylphenyl)-5-(4-chlorophenylsulfonyl)-1,3-oxazol-4-ylphosphonic acid* was 76%. M.p. 197−199 °C. IR (KBr): ν cm^{-1} 1312 (SO$_2$), 1150 (SO$_2$), 1208 (P=O). ^{1}H NMR (DMSO-d$_6$): (δ ppm) 8.23, 7.91, 7.78, 7.42 (m, 8H, 2C$_6$H$_4$), 4.04 (m, 2H, CH$_2$), 2.39 (s, 3H, CH$_3$), 1.23 (t, 3H, CH$_3$). ^{31}P NMR (DMSO-d$_6$): (δ ppm) 4.9. Anal. Calcd. for C$_{18}$H$_{17}$ClNO$_6$PS: Cl, 8.02; N, 3.17; P, 7.01; S 7.26; Found: Cl, 8.22; N, 3.01; P, 7.28; S, 7.35. Sodium salt **6** was prepared by evaporation to dryness under a reduced pressure of mixture aqueous solution of 1 mmol of acid and 1 mmol of sodium bicarbonate which used without further purification for biological tests.

2.2. Antifungal activity

The fungi *C. albicans* M885 (ATCC 10231) and its clinical isolate were used as tested microorganisms. The strains were subcultured on Sabouraud agar in Petri plates according to the manufacturer's instructions. The standard agar disk diffusion method [16] was performed to evaluate anti-Candida property of studied compounds. Compounds concentration was 2,0 and 20,0 μM. The microbial loading made $1 \cdot 10^5$ CFU/mL. The incubation period was 24 h at 37 °C. Compounds were considered active if the diameter of zones growth inhibition of fungi culture was more than 15 mm.

2.3. Search, selection and sequence alignment of FBA-II

In the work, the sequences of FBA-II *M. tuberculosis* (strain ATCC 25618/H37Rv) (UniProt: P9WQA3) [17] and FBA-II *C. albicans* (strain SC5314/ATCC MYA-2876) (UniProt: Q9URB4) [18] were used. The amino acid sequence of FBA-IIs *C. albicans* and *M. tuberculosis* were sequence-aligned using the Needleman-Wunsch Global Align Protein Sequences (NCBI) [19] with applying BLOSUM-62 matrix and Gap costs (11,1).

2.4. Protein model creation and validation

SWISSMODEL server [20] was used for FBA-II *C. albicans* sequence (UniProt: Q9URB4) modeling. First, a preliminary search for evolutionarily related sequences was performed using the SWISS-MODEL Template Library. The searching was conducted by BLAST [21] and HHBlits [22] for structures analysis of similar to FBA-II *C. albicans* sequence. Secondly, homology models were created based on the results ranking of the templates. The homology models quality validation of FBA-II *C. albicans* was conducted by ERRAT and PROCHECK. ERRAT [23] was used for the unrelated interactions statistic between different atoms types and error function value graphs in comparison with the position of the sliding window with 9 residues, calculated considering the highly purified structures statistic. PRO-CHECK was used for the stereochemical quality verification of a protein structure by analyzing residue-by- residue geometry and overall structure geometry [24].

2.5. Molecular docking

Minimized and validated model FBA-II *C. albicans* was used for the protein-ligand docking studies. The molecular docking was conducted similar to our earlier works [25, 26, 27]. The docking compatible structures of the protein, ligands and grid box creation were made by using AutoDock Tools (ADT) (ver.1.5.6) [28].The structure of FBA-II A-subunit was selected and stored as a PDB file by Accelrys DS (ver. 2.5.5) [29]. All protein hydrogens were added using ADT and no Bond Order method and the macromolecule atoms were renumbered including the new hydrogens. The partial charges were calculated and added by using Gasteiger method and the prepared protein structure was saved in PDBQT format.

The structures and conformations of studied ligands were created by using Chem-Axon Marvin Sketch 5.3.735 [30] and were saved in Mol2 format. The optimization of the ligands structures and energy minimization were performed by software Avogadro v1.1.1 [31]. We used the "Auto Optimization Tool" by applying the MMFF94s force field and the steepest descent algorithm. Partial charges and torsions angles of ligands were changed by ADT and the ligand structures were saved as the resulting files in PDBQT format.

The prepared protein structure and optimized ligands were used for the conduction of docking simulations by AutoDock 4.2 [32]. Lamarckian genetic algorithm method and standard docking procedure for the rigid protein were used. The ADT was used to generate of the docking parameter files and both grid. Zn atom was set as the box center. The grid map of 50*50*50 points with grid spacing of 0.375 Å was used and the settings for other parameters were applied by default. The molecular docking time of one ligand was about 30 min. All operations were made on Windows XP SP3 computer with an Intel Core i3 CPU (3.20 GHz) and 2 GB of RAM. The software package Accelrys DS was used for illustration and to analyze the protein−ligand interactions.

3. Results and discussion

Our assumption about the phosphonates contained inhibitors of FBA-II *C. albicans* is confirmed by the existence of FBP, DHAP and PGH analogues with high inhibitory activity to this enzyme [33]. It should also be noted that one of the most studied FBA-II is the FBA-II *M. tuberculosis* [34]. A number of large bioassays containing inhibitors of the FBA-II *M. tuberculosis* are available on the Pubchem server - PubChem AID: 588726 [35], 651616 [36], 652141 [37].

3.1. Alignment of FBA-II *C. albicans* and FBA-II *M. tuberculosis* protein sequences

Structural analogy was used for the development of FBA-II *C. albicans* inhibitors. FBA-IIs *C. albicans* and *M. tuberculosis* were analyzed using Protein BLAST (NCBI) - Needleman-Wunsch Global Align Protein Sequences [19]. Sequences of FBA-II *C. albicans* and FBA-II *M. tuberculosis* were used for comparing in accordingly to the substitution Matrix (BLOSUM-62) and Gap Costs (11,1) operating parameters (Fig. 1).

The obtained results (Fig. 1) indicate about the significant enzymes similarity of the organisms. So, the sequence identities was 41%, the sequence similarity was 55% and a number to gaps was 9%. These results confirmed the high similarity of enzyme primary structures.

The secondary structure similarity, the binding sites and the active sites of FBA-IIs were analyzed by Accelrys DS (Fig. 2).

Fig. 2 has demonstrated a significant similarity not only primary but also secondary structure of enzymes. The similarity is noted in the area of metal binding sites, active sites and DHAP, GAP binding sites.

Thus, the established significant similarity of enzyme structures assumes the inhibitors structural similarity.

```
NW Score        Identities              Positives               Gaps
547             152/369(41%)            204/369(55%)            35/369(9%)

Query  1    MPIATPEVYA-----------EMLGQAKQNSYAFPAINCTSSETVNAAIKGFADAGSDGI  49
            M  A P V +            ++   A++  +A PAIN TSS TV AA++   D + I
Sbjct  1    M--APPAVLSKSGVIYGKDVKDLFDYAQEKGFAIPAINVTSSSTVVAALEAARDNKAPII  58

Query  50   IQFSTGGAEFGSGLGV--KDM---VTGAVALAEFTHVIAAKYPVNVALHTDHCPKDKLDS  104
            +Q S GGA + +G GV  KD     + G++A A +  IA  Y + V LHTDHC K KL
Sbjct  59   LQTSQGGAAYFAGKGVDNKDQAASIAGSIAAAHYIRAIAPTYGIPVVLHTDHCAK-KLLP  117

Query  105  YVRPLLAISAQRVSKGGNPLFQSHMWDGSAVPIDENLAIAQELLKAAAAAKIILEIEIGV  164
            +    +L   +  +K G PLF SHM D S    DEN+A  +  + A    LE+EIG+
Sbjct  118  WFDGMLKADEEFFAKTGTPLFSSHMLDLSEETDDENIATCAKYFERMAKMGQWLEMEIGI  177

Query  165  VGGEEDGVANEINEK--LYTSPEDFEKTIEALGAGEHGKYLLAATFGNVHGVYKPGNVKL  222
             GGEEDGV NE  EK  LYTSPE     E+L       + +AA FGNVHGVYKPGNV+L
Sbjct  178  TGGEEDGVNNEHVEKDALYTSPETVFAVYESLHKISPN-FSIAAAFGNVHGVYKPGNVQL  236

Query  223  RPDILAQGQQVAAAKLGLPADAK-PFDFVFHGGSGSLKSEIEEALRYGVVKMNVDTDTQY  281
            RP+IL   Q  A  ++G    DAK P   VFHGGSGS + E   A++ GVVK+N+DTD QY
Sbjct  237  RPEILGDHQVYAKKQIG--TDAKHPLYLVFHGGSGSTQEFNTAIKNGVVKVNLDTDCQY  294

Query  282  AFTRPIAGHMFTNYDGVLK--VDGEVGV----KKVYDPRSYLKKAEASMSQRVVQACNDL  335
            A+  I  ++ TN   LK  V   G      KK +DPR ++++ E +MS+R+ +A +
Sbjct  295  AYLTGIRDYV-TNKIEYLKAPVGNPEGADKPNKKYFDPRVWVREGEKTMSKRIAEALDIF  353

Query  336  HCAGKSLTH  344
            H   G+
Sbjct  354  HTKGQL     359
```

Fig. 1. Protein BLAST results of FBA-II *C. albicans* (359) and FBA-II *M. tuberculosis* (344) by application of Needleman-Wunsch Global Align Protein Sequences.

3.2. Development of FBA-II *C. albicans* inhibitors

The BioAssay 588726 was used as BioAssay with the greatest number of FBA-II *M. tuberculosis* inhibitors − 8221 compounds. Analysis of inhibitor structures by Chemaxon Instant JChem [38] allowed to identify 333 inhibitors as 1,3-oxazole derivatives and 25 compounds as 1,3-oxazole-4-phosphonate derivatives (Fig. 3).

Thus, it is established, that 25 FBA-II *M. tuberculosis* inhibitors contains the 1,3-oxazole-4-phosphonate moiety in the structure (Fig. 4). So, design of FBA-II *C. albicans* inhibitors was performed by analogy of FBA-II *M. tuberculosis* inhibitors containing this moiety. One group of 1,3-oxazole-4-phosphonates inhibitors was modified at the C2 position to make 2-methyl- and 2-methylphenyloxazole
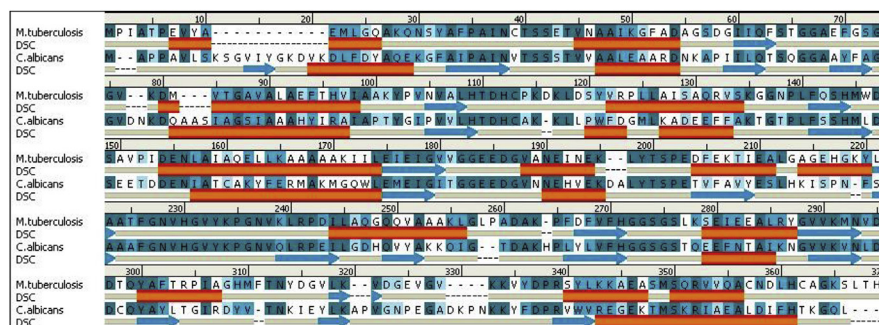
Fig. 2. A comparison of secondary structure, binding sites and active sites of FBA-II *C. albicans* and FBA-II *M. tuberculosis* by Accelrys DS.

Pubchem Bioassay (AID:588726),
8221 compounds total

333 of them is 1,3-oxazole-based
compounds

25 of them is 1,3-oxazole-4-
phosphonates compounds
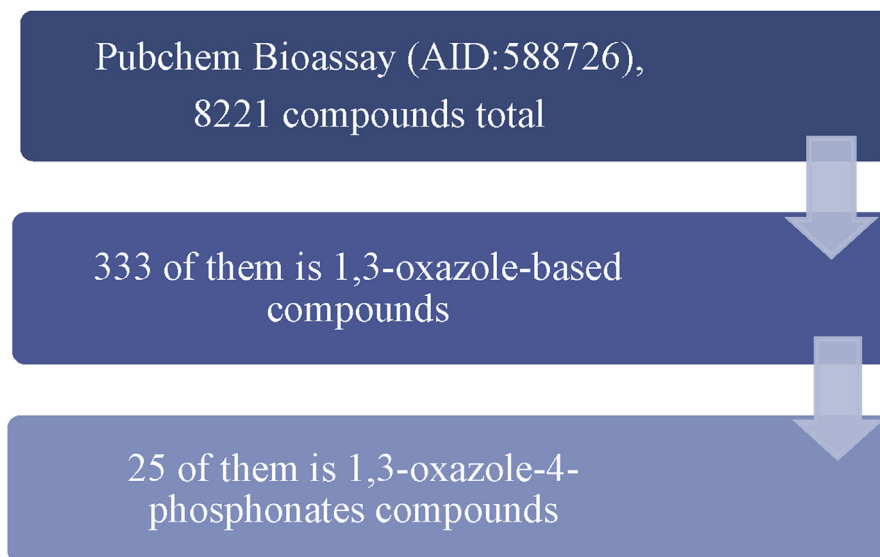
Fig. 3. Analysis of FBA-II *M. tuberculosis* inhibitors structures (PubChem bioassay AID: 588726). The structures of some FBA-II *M. tuberculosis* inhibitors from PubChem AID: 588726 are shown in Fig. 4.

derivatives and at the C5 position to form 5-carboxypiperidine derivatives. Second group of 1,3-oxazole-4-phosphonate inhibitors was modified at the C2 position to give 2-methylbenzoxazoles and at the C5 position to form 5-methylphenylsulfonyl and 5-chlorophenylsulfanyl derivatives. Designed compounds 1−6 were synthesized for biologycal testing (Fig. 5).

3.3. Antifungal evaluation

Anti-Candida activity results of the studied compounds against fungi *C. albicans* M885 (ATCC 10231) and fluconazole (FCZ) resistance *C. albicans* clinical isolate are presented in Table 1.
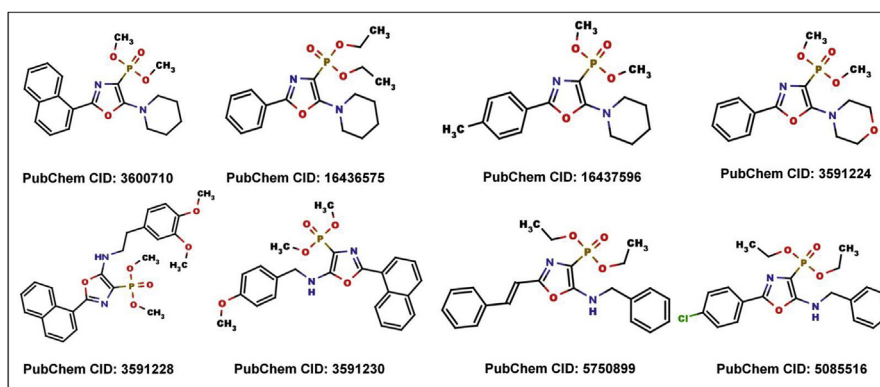
Fig. 4. Structures of FBA-II *M. tuberculosis* inhibitors from the PubChem bioassay AID:588726.
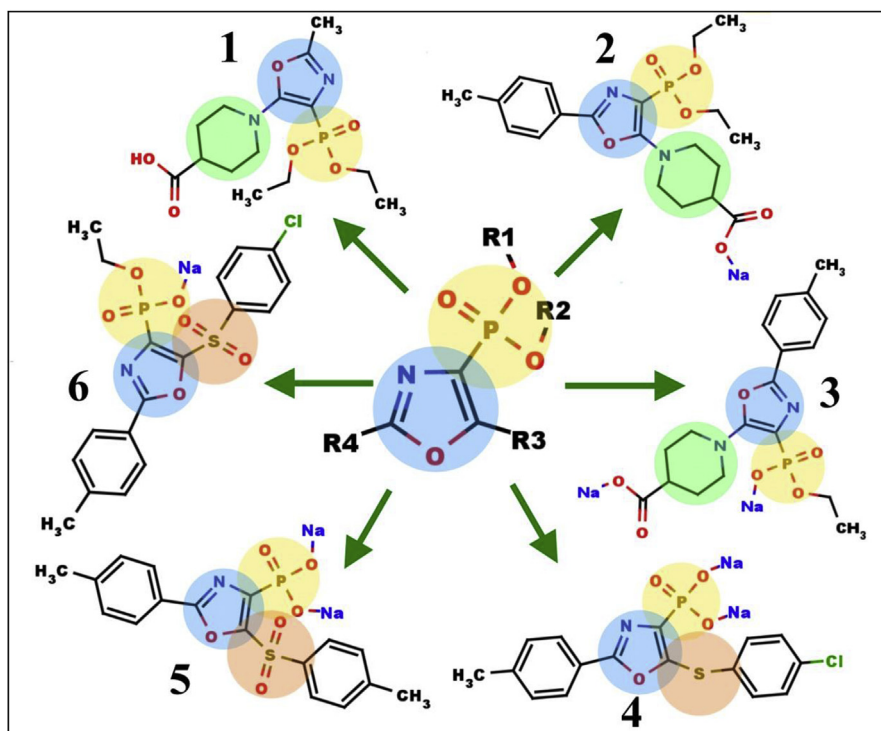
Fig. 5. Design of the 1,3-oxazole-4-phosphonate derivatives as active FBA-II *C. albicans* inhibitors.

Table 1 shows that all studied compounds had fluconazole-like activity against *C. albicans* M885 (ATCC 10231) in both applicable concentration. Activity of the studied compounds in applicable concentrations 2,0 μM against *C. albicans* clinical isolate as the diameters of inhibition zone around the all compounds disks didn't

Table 1. Anti-Candida activity of the studied compounds.

Compound	Applicable concentration, μM	*Candida albicans* M885(ATCC 10231)	clinical isolate of *Candida albicans*
1	2,0	20,7	11,0
	20,0	27,3	16,8
2	2,0	22,2	9,3
	20,0	25,9	17,1
3	2,0	22,7	10,3
	20,0	27,2	17,5
4	2,0	21,3	11,0
	20,0	26,6	18,1
5	2,0	23,0	9,0
	20,0	26,6	17,0
6	2,0	23,3	10,5
	20,0	26,2	16,9
FCZ	2,0	1,5	H/A
	20,0	26,7	H/A

exceed 11 mm and 18 mm in applicable concentration 20,0 μM. It's important that fluconazole wasn't active in both applicable concentrations.

We have assumed that the inhibiting action mechanism of 4-phosphorylated derivatives of 1,3-oxazole against the fluconazole-resistant *C. albicans* clinical isolate strain can be connected not with 14α-demethylase inhibition like an flukonazol, but with other fungal molecular target.

3.4. Protein modelling

3.4.1. Creating of FBA-II C. albicans *homology 3D model*

The preliminary search of the FBA-II related sequences was performed using SWISS-MODEL Template Library and 36 templates were created (Supplementary Material). 10 templates (Fig. 6) with a sequence identity above 49% were selected and 10 models were built based on this templates (Table 2).

Based on the sequence identity value, QSQE and resolution, three most significant enzyme models such as #10 (3qm3.1.A), #01 (1b57.1.A) and #03 (5gk3, 1.A) were selected and presented in Figs. 7, 8, and 9.

3.4.2. Quality evaluation of the built FBA-II C. albicans *homology 3D model*

The quality estimation of the model #10 selected as optimal FBA-II *C. albicans* model was conducted by using ERRAT and PROCHECK. ERRAT-web server results showed the high model quality. The overall quality factor for the subunit A was 98.780 and for the subunit B was 97.953 (Figs. 10 and 11).

Template Results

	Name	Title	Coverage	GMQE	QSQE	Identity	Method	Oligo State	Ligands
☑	1b57.1.A	PROTEIN (FRUCTOSE-BISPHOSPHATE ALDOLASE II)		0.77	0.73	54.84	X-ray, 2.0Å	homo-dimer ✓	7 x ZN, 2 x PGH
☑	1zen.1.A	CLASS II FRUCTOSE-1,6-BISPHOSPHATE ALDOLASE		0.76	0.69	54.84	X-ray, 2.5Å	homo-dimer ✓	4 x ZN
☑	5gk3.1.A	Fructose-bisphosphate aldolase class 2		0.76	0.73	54.84	X-ray, 1.8Å	homo-dimer ✓	2 x ZN
☑	1b57.1.A	PROTEIN (FRUCTOSE-BISPHOSPHATE ALDOLASE II)		0.77	0.76	53.41	X-ray, 2.0Å	homo-dimer ✓	7 x ZN, 2 x PGH
☑	1zen.1.A	CLASS II FRUCTOSE-1,6-BISPHOSPHATE ALDOLASE		0.76	0.71	53.41	X-ray, 2.5Å	homo-dimer ✓	4 x ZN
☑	5gk3.1.A	Fructose-bisphosphate aldolase class 2		0.77	0.75	53.26	X-ray, 1.8Å	homo-dimer ✓	2 x ZN
☑	1dos.1.A	ALDOLASE CLASS II		0.78	0.74	53.12	X-ray, 1.7Å	homo-dimer ✓	2 x ZN
☑	1dos.1.B	ALDOLASE CLASS II		0.78	0.74	53.12	X-ray, 1.7Å	homo-dimer ✓	2 x ZN
☑	3qm3.1.A	Fructose-bisphosphate aldolase		0.77	0.76	50.15	X-ray, 1.8Å	homo-dimer ✓	2 x ZN
☑	3qm3.1.A	Fructose-bisphosphate aldolase		0.77	0.78	49.00	X-ray, 1.8Å	homo-dimer ✓	2 x ZN

Fig. 6. Selected templates for models building.

Table 2. Qualitative indicators of created 10 homology models.

Template	Sequence Identity	Oligo-state	QSQE	Found by	Method	Resolution, Å	Sequence Similarity	Coverage	Description
3qm3.1.A	49.00	homo-dimer	0.78	HHblits	X-ray	1.85	0.45	0.97	Fructose-bisphosphate aldolase class II
3qm3.1.A	50.15	homo-dimer	0.76	BLAST	X-ray	1.85	0.45	0.95	Fructose-bisphosphate aldolase class II
1b57.1.A	53.41	homo-dimer	0.76	HHblits	X-ray	2.00	0.45	0.98	Fructose-bisphosphate aldolase II
5gk3.1.A	53.26	homo-dimer	0.75	HHblits	X-ray	1.80	0.45	0.98	Fructose-bisphosphate aldolase class II
1dos.1.A	53.13	homo-dimer	0.74	HHblits	X-ray	1.67	0.45	0.98	Fructose-bisphosphate aldolase class II
1dos.1.A	53.13	homo-dimer	0.74	HHblits	X-ray	1.67	0.45	0.98	Fructose-bisphosphate aldolase class II
1b57.1.A	54.84	homo-dimer	0.73	BLAST	X-ray	2.00	0.46	0.95	Fructose-bisphosphate aldolase class II
5gk3.1.A	54.84	homo-dimer	0.73	BLAST	X-ray	1.80	0.45	0.95	Fructose-bisphosphate aldolase class II
1zen.1.A	53.41	homo-dimer	0.71	HHblits	X-ray	2.50	0.46	0.98	Fructose-bisphosphate aldolase class II
1zen.1.A	54.84	homo-dimer	0.69	BLAST	X-ray	2.50	0.46	0.95	Fructose-bisphosphate aldolase class II
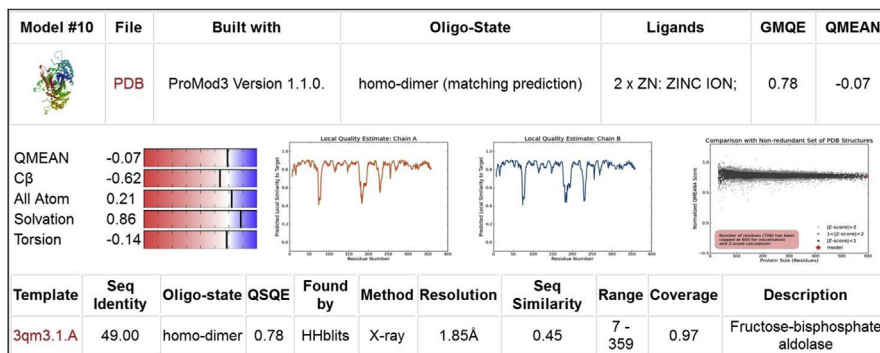
Fig. 7. Quality of the built model #10.

PROCHECK-web server data analysis has been also confirmed the 3D model structure FBA-II good quality by using Ramachandran plot analysis (Fig. 12).

Ramachandran plot results indicated that 92.3 % of the protein residues were distributed in the favored regions, 7.2 % - in the additionally allowed regions, 0.5 % - in the generously allowed regions and the absent of residues in the disallowed region. Thus, the created 3D structure of FBA-II C. *albicans* is adequate and can be used for the molecular docking.

3.5. Molecular docking

Molecular docking of the compounds **1−6** to the active site of FBA-II C. *albicans* were performed for mechanism interpretation of the high antifungal activity of studied compounds.

3.5.1. Identification of FBA-II C. albicans inhibitors binding modes

The similarity of the protein structure of FBA-II *C. albicans* and FBA-II *M. tuberculosis* was used for searching binding site of the studied compounds. The obtained

Fig. 8. Quality of the built model #01.

Model #03	File	Built with	Oligo-State	Ligands	GMQE	QMEAN
	PDB	ProMod3 Version 1.1.0.	homo-dimer (matching prediction)	2 x ZN: ZINC ION;	0.76	-0.56

QMEAN	-0.56		
Cβ	-1.06		
All Atom	0.45		
Solvation	0.90		
Torsion	-0.57		

Template	Seq Identity	Oligo-state	QSQE	Found by	Method	Resolution	Seq Similarity	Range	Coverage	Description
5gk3.1.A	54.84	homo-dimer	0.73	BLAST	X-ray	1.80Å	0.46	9 - 350	0.95	Fructose-bisphosphate aldolase class 2
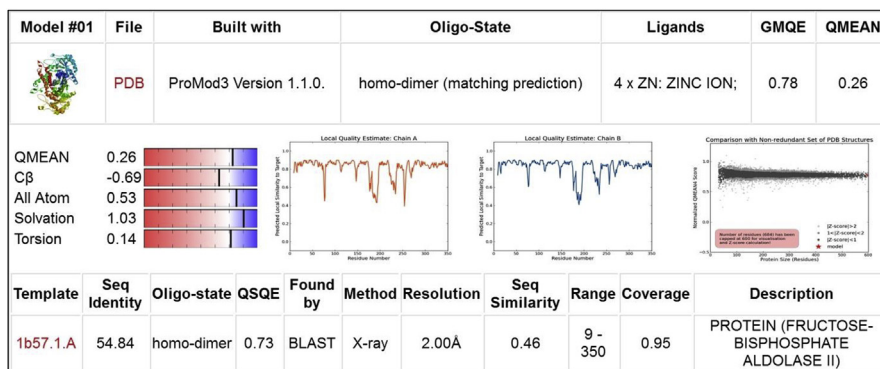
Fig. 9. Quality of the built model #03. In our opinion, model #10 is the most optimal considering the values of resolution (1.85Å), QMEAN (-0.07), GMQE (0.78), GSQE (0.78) indicators.

sequence identity indicator (41%) and sequence similarity indicator (55%) (Fig. 1) confirm the significant similarity of protein structures of enzymes, analogically to Han X. et al. [33]. To search of the enzyme inhibitors optimal binding center, a number of FBA-II *M. tuberculosis* crystallographic structure [34, 39] were used. The location of the enzyme-related inhibitors and the character of **FBP** binding in FBA-II catalytic center were investigated. As a result of the crystallographic structures analysis, it was shown that the inhibitors binding site is in the region of the ione Zn (II). The key role of the divalent metal ion for the ketocarbonyl group polarization of the substrate and the enoanolate stabilization has been experimentally confirmed earlier [34, 40, 41]. Thus, the zinc atom with coordinates (x = 52,103, y = 56,243, z = 92,751) can be the docking center of inhibitors FBA-II *C. albicans* similarly to FBA-II *M. tuberculosis*.

3.5.2. The molecular docking procedure of studied 1,3-oxazole-4-phosphonates derivatives

Molecular docking experiments of FBA-II *C. albicans* with 1,3-oxazole-4-phosphonates were performed using AutoDock Tools software (Figs. 13, 14, 15, 16, and 17).

Molecular docking of ligand **3** (Fig. 13) to the active site of FBA-II showed that the phosphonate group forms three electrostatic bonds of length 5.12Å, 4.02Å and 4.82Å with a catalytic zinc atom and amino acid residues His110 (Pi-anion) and Asp144, and two hydrogen bonds of length 3.64Å and 2.83 Å with amino acid residues Gly227 and Val228.

The oxazole ring forms an electrostatic Pi-anion bond of length 3.18Å with amino acid residue Asp144, and a hydrophobic Pi-alkyl bond of length 5.35Å with Ala112.
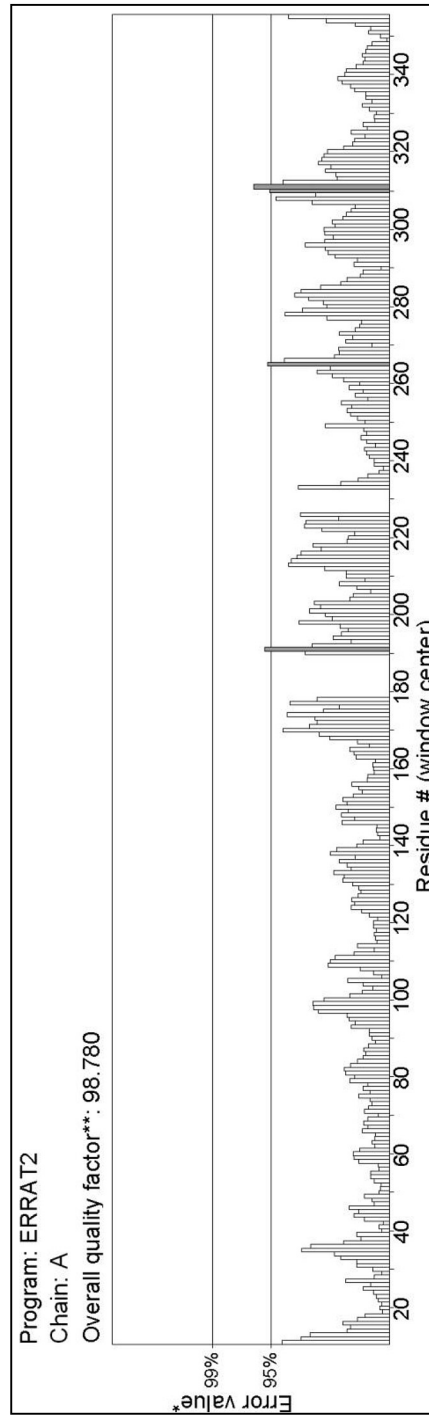
Fig. 10. The 3D profile of subunit A FBA-II *C. albicans* verified by using ERRAT server.
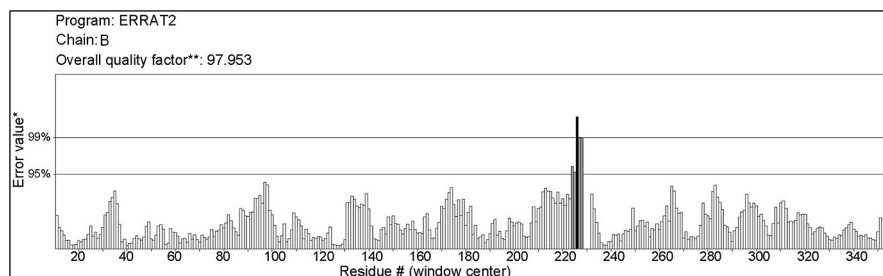
Fig. 11. The 3D profile of subunit B FBA-II *C.albicans* verified by using ERRAT server.

The piperidine ring forms a hydrogen bond of length 3.62Å with Glu147, and a hydrophobic Pi-alkyl bond of length 4.76Å with the key amino acid His226.

The formation of two hydrogen bonds of 3.20Å and 3.33Å length between the carboxyl group and His226 and Val225, and of one electrostatic bond of length 4.57Å with Lys230 should also be mentioned.

There are also two hydrophobic (alkyl and Pi-sigma) bonds of length 3.50Å and 4.88Å between the aromatic ring and ring methyl group and the Ala112 and Leu145.

Molecular docking of ligand **4** (Fig. 14) to the enzyme binding site demonstrates the formation of five electrostatic bonds with phosphonate moiety of length 1.75 Å, 3.55 Å, 3.57 Å, 3.62 Å, 4.04Å with a catalytic zinc atom, His110, Asp144 and of one hydrogen bond of length 2.60Å with amino acid residue His226.
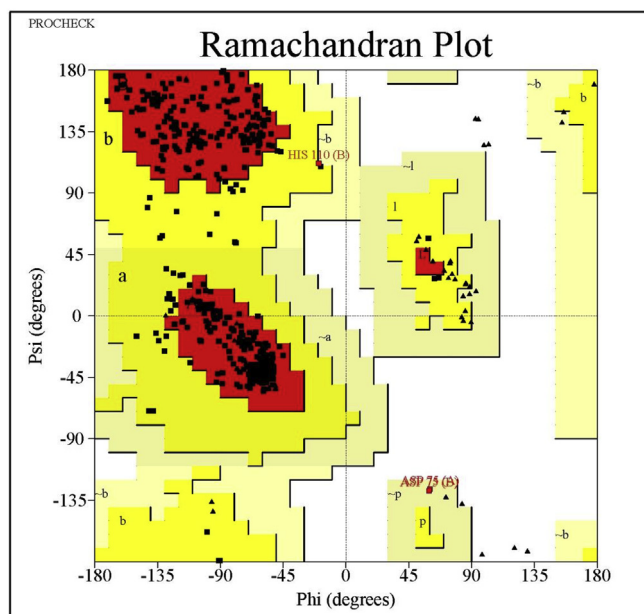
Fig. 12. Ramachandran plot of the stereochemical quality of FBA II *C.albicans* model generated by PROCHECK validation server.
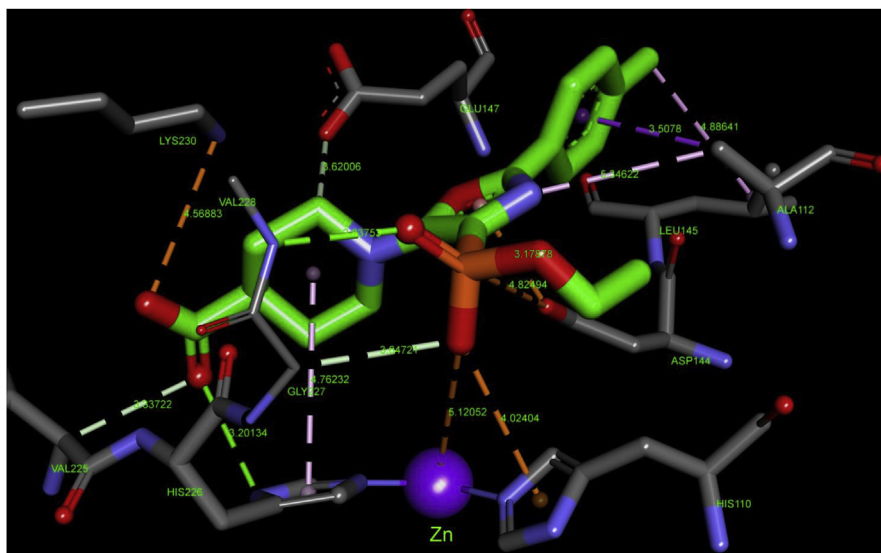
Fig. 13. Molecular docking of compound **3** into the active site of FBA-II *C. albicans*.

The first aromatic ring forms one electrostatic Pi bond of length 3.30Å with amino acid Asp144, two hydrophobic Pi-sigma bonds of length 3.55Å and 5.35 Å with Ala112, and a halogen bond of length 3.00Å between Asp144 and ring chlorine atom.

The oxazole ring forms a hydrophobic Pi-Pi bond of length 3.96Å with amino acid residue His226. There are also three hydrophobic alkyl and Pi-sigma bonds of length 3.73Å, 4.17Å and 4.62Å between the second aromatic ring and amino acids Asn224 and Val225.

Molecular docking of ligand **5** shown in Fig. 15 indicates the presence of 4.42Å, 5.40Å 3.91Å, 4.53Å, 4.80Å and 4.65Å long electrostatic bonds between the
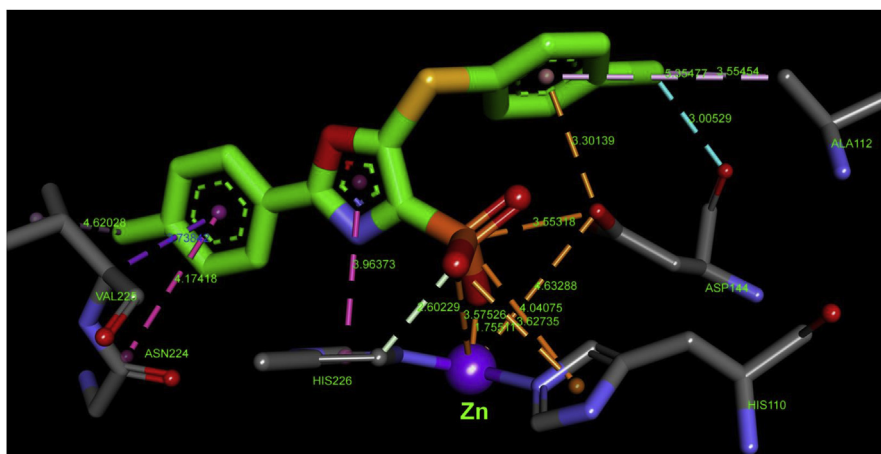
Fig. 14. Molecular docking of compound **4** into the FBA-II *C. albicans* active site.
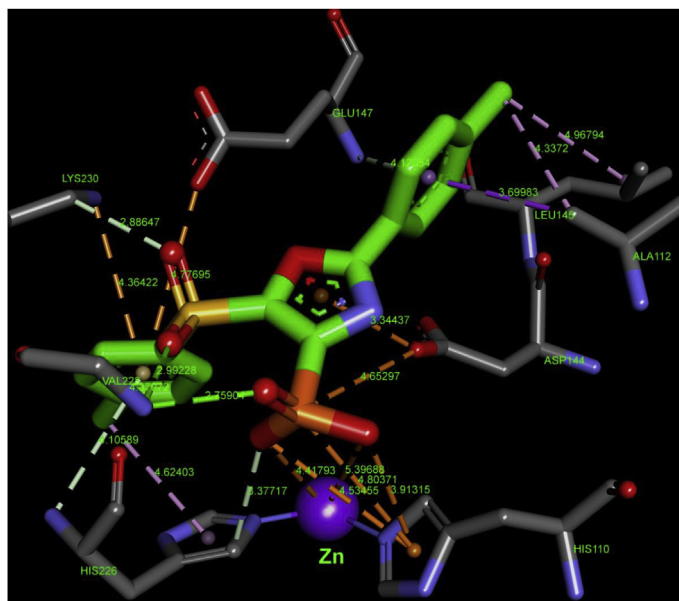
Fig. 15. Molecular docking of compound **5** into the active site of FBA-II *C. albicans*.

phosphonate group and catalytic zinc atom, amino acid residues His110 and Asp144 respectively, and of 2.75Å, 3.37Å long hydrogen bonds with His226 and Val228. The oxazole ring forms an electrostatic bond of length 3.34Å with Asp144.
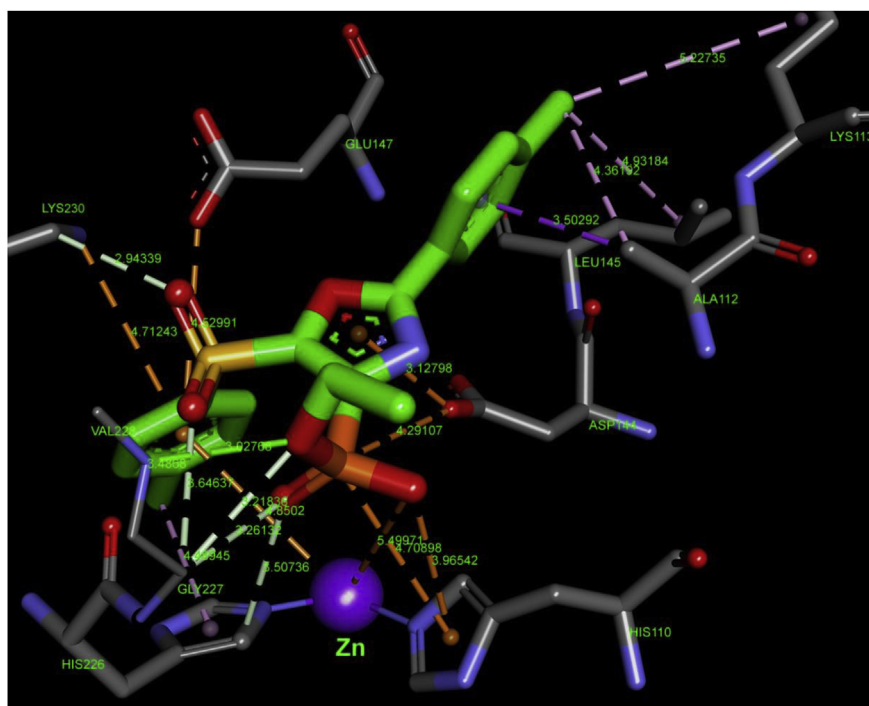
Fig. 16. Molecular docking of compound **6** into the active site of FBA-II *C. albicans*.
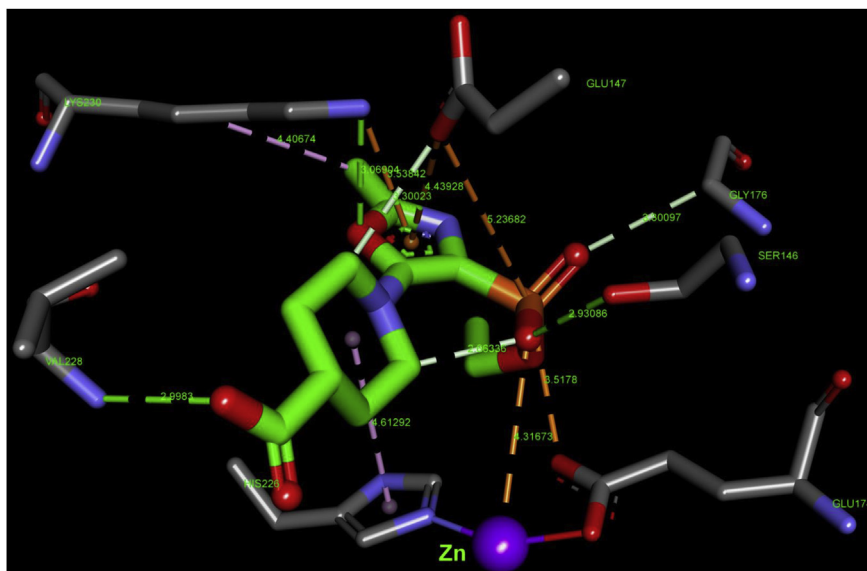
Fig. 17. Molecular docking of compound **1** into the active site of FBA-II *C. albicans*.

Formation of two electrostatic Pi bonds of length 4.38Å and 4.77Å is shown between amino acid Lys230, Glu147 and of first aromatic ring. Also, the ring methyl group forms a hydrophobic Pi-alkyl bond of length 4.62Å with His226.

The sulfonyl group forms two hydrogen bonds of length 2.88Å and 2.99 Å with Lys230 and Val228. The second aromatic ring forms three hydrophobic alkyl and Pi-sigma bonds of length 3.69Å, 4.33Å and 4.96Å with Ala112 and Leu145 and one hydrogen bond of length 4.12Å with Glu147.

Molecular docking of ligand **6** (Fig. 16) to the active site of FBA-II indicates the formation of four electrostatic bonds of length 3.96Å, 4.70Å, 4.29 Å and 5.50Å between phosphonate group and amino acid residues His110, Asp144 and catalytic zinc atom, also the formation of four hydrogen bonds of length 3.50Å, 3.26Å, 3.21Å and 3.02Å with amino acid residues His226, Gly227 and Val228.

The oxazole ring forms only electrostatic Pi-anion bond of length 3.12Å with Asp144.

Three electrostatic Pi bonds of length 4.85Å, 4.73Å and 4.53 Å with catalytic zinc atom and Lys230, Glu147 has been formed by first aromatic ring and chlorine atom forms a hydrophobic Pi-alkyl bond of length 4.49Å with His226.

Also, the sulfonyl group forms two hydrogen bonds of length 3.64Å and 2.94 Å with Gly227 and Lys230. The second aromatic ring forms four hydrophobic alkyl and Pi-sigma bonds of length 3.50Å, 4.36Å, 4.93Å and 5.23Å with Ala112, Leu145 and Lys113 respectively.

Molecular docking of compounds **1** and **2** into the *C. albicans* FBA-II active center showed the formation of low-energy ligand-protein complexes and ligands localization at long distance from the catalytic zinc atom (>6Å). Therefore, based on the significant structural similarity and similarity of the level of anti-Candida activity of compounds **1**−**3**, it was suggested that the hydrolysis of dialkylphosphonates **1** and **2** to monoalkylphosphonates in the course of interaction with the *C. albicans* enzyme system is possible [42, 43, 44, 45, 46]. Thus, compounds **1** and **2** were docked as monoesters. Molecular docking of compound **2** as a monoalkylphosphonate has demonstrated the results similar to the compound **3** (Fig. 13).

Molecular docking of ligand **1** (Fig. 17) into the active site of FBA-II shown the formation of three electrostatic bonds of length 3.52Å, 4.37Å, 5.24Å between phosphonate group and amino acid residues Glu174, Glu147 and catalytic zinc atom, and of two hydrogen bonds of length 2.93Å, 3.30Å between phosphonate group and amino acid residues Gly176, Ser146.

Formation of two electrostatic Pi bonds of length 4.44Å, 3.30Å between the oxazole ring and Glu147, Lys230, of hydrogen bond of length 3.07Å between the oxazole ring and Lys230, of hydrophobic Pi bond of length 4.40Å between the oxazole ring and Lys230 is shown.

The piperidine ring forms a hydrogen bond of length 3.30Å with Glu147 and a hydrophobic Pi-alkyl bond of length 4.61Å with the key amino acid His226. There is also a hydrogen bond of length 2.99Å between the carboxyl group and amino acid residue Val228.

The result of the molecular docking of all ligands has shown that all tested compounds has common type of interaction with the catalytic center of the enzyme through the phosphonate group. High stability of ligand-protein complexes formed by compounds **1**−**6** with binding energy ΔG = −6.89, −7.2, −7.16, −7.5, −8.0, −7.9 kcal/mol respectively is demonstrated. The amino acid residues His110, His226, Gly227, Leu248, Val238, Asp144, Lys230, Glu174, Glu147, Gly227, Ala112, Leu145 and catalytic zinc atom performs the key role in the binding of these compounds in the FBA-II active site *C. albicans*.

4. Conclusions

The synthesis, *in vitro* antifungal activity and molecular modelling of 4-phosphorylated derivatives of 1,3-oxazole as inhibitors of *C. albicans* fructose-1,6-bisphosphate aldolase were performed and discussed.

The structure similarity of FBA-II *C. albicans* and FBA-II *M. tuberculosis* was the basis of the strategy for the design of new anti-Candida agents as fructose-1,6-bisphosphate aldolase inhibitors.

A significant similarity of the FBA-II *C. albicans* and FBA-II *M. tuberculosis* is shown using NCBI Protein BLAST with the application of Needleman-Wunsch Global Align Protein Sequences. Also, a similarity of secondary structure, metal binding sites, active sites and substrate binding sites of these enzymes were demonstrated by DS.

FBA-II *C. albicans* inhibitors were developed and synthesized based on the structure similarity of FBA-II *M. tuberculosis* inhibitors contained 1,3-oxazole-4-phosphonates moiety.

The experimental studies of the anti-Candida activity shown the high antifungal potential of studied compounds against *C. albicans* M885 (ATCC 10231). The established growth inhibition of fluconazole-insensitive clinical isolate was connected with fructose-1,6-bisphosphate aldolase inhibition. To confirm the proposed action mechanism FBA-II *C. albicans* homology model was created using the SWISS-MODEL server. High quality of the created homology model was confirmed by using ERRAT and PROCHECK.

The presumed mechanism of inhibition by studied compounds was demonstrated using molecular docking into the active site of FBA-II *C. albicans* homology model. Molecular docking analysis showed the key role of amino acid residues His110, His226, Gly227, Leu248, Val238, Asp144, Lys230, Glu147, Gly227, Ala112, Leu145 and catalytic zinc atom in the binding of compounds into the *C. albicans* FBA-II active site. The high stability of ligand-protein complexes is ensured by electrostatic bonds, H-bonds, Pi-Sigma bonds, Pi-alkyl and alkyl interactions and is confirmed by high binding energy with $\Delta G = -6.89, -7.2, -7.16, -7.5, -8.0, -7.9$ kcal/mol. It has been shown that the phosphonate group forms the multiple electrostatic and hydrogen bonds at the FBA-II binding site with zinc atom and amino acid residues His110, His226 and Asp144.

Thus, a qualitative homology model of *C. albicans* FBA-II can be used as a new tool for the construction of new anti-Candida agents with specific action mechanism. 4-phosphorylated derivatives of 1,3-oxazole are a promising drug candidates for the development of new antifungal agents against fluconazole-insensitive clinical isolate *C. albicans*.

Declarations

Author contribution statement

Ivan Semenyuta: Conceived and designed the experiments; Performed the experiments; Analyzed and interpreted the data; Contributed reagents, materials, analysis tools or data; Wrote the paper.

Funding statement

Competing interest statement

The authors declare no conflict of interest.

Additional information

Supplementary content related to this article has been published online at https://doi.org/10.1016/j.heliyon.2019.e01462.

Acknowledgements

References

[1] D.A. Enoch, H. Yang, S.H. Aliyu, C. Micallef, The changing epidemiology of invasive fungal infections, Methods Mol. Biol. 1508 (2017) 17−65.

[2] T.P. Salci, M. Negri, A.K.R. Abadio, T.I.E. Svidzinski, E.S. Kioshima, Targeting *Candida spp*. to develop antifungal agents, Drug Discov. Today 23 (2018) 802−814.

[3] W.E. Goldman, A. Butts, D.J. Krysan, Antifungal drug discovery: something old and something, New PLoS Pathog. 8 (2012) 70−73.

[4] S.C. Chen, M.A. Slavin, T.C. Sorrell, Echinocandin antifungal drugs in fungal infections: a comparison, Drugs 71 (2011) 11−41.

[5] J. Brajtburg, W.G. Powderly, G. S Kobayashi, G. Medoff, Amphotericin B: current understanding of the mechanisms of action, Antimicrob. Agents Chemother. 34 (1990) 183−188.

[6] A. Vermes, H.J. Guchelaar, J. Dankert, Flucytosine: a review of its pharmacology, clinical indications, pharmacokinetics, toxicity and drug interactions, J. Antimicrob. Chemother. 46 (2000) 171−179.

[7] W. Zhang, Y. Ramamoorthy, T. Kilicarslan, H. Nolte, R.F. Tyndale, E.M. Sellers, Inhibition of cytochromes P450 by antifungal imidazole derivatives, Drug Metab, Dispos 30 (2002) 314−318.

[8] W.J. Rutter, Evolution of aldolase, fed, SAVE Proc. 23 (1964) 48−57.

[9] A. Rodaki, T. Young, A.J. Brown, Effects of depleting the essential central metabolic enzyme fructose-1,6-bisphosphate aldolase on the growth and viability of *Candida albicans*: implications for antifungal drug target discovery, Eukaryot. Cell 8 (2006) 71−77.

[10] M. de la Paz Santangelo, P.M. Gest, M.E. Guerin, M. Coinçon, H. Pham, G. Ryan, S.E. Puckett, J.S. Spencer, M. Gonzalez-Juarrero, R. Daher, A.J. Lenaerts, D. Schnappinger, M. Therisod, S. Ehrt, J. Sygusch, M. Jackson, Glycolytic and non-glycolytic functions of *Mycobacterium tuberculosis* fructose-1,6-bisphosphate aldolase, an essential enzyme produced by replicating and non-replicating bacilli, J. Biol. Chem. 46 (2011) 219−231.

[11] T. Doan, S. Aymerich, Regulation of the central glycolytic genes in *Bacillus subtilis*: binding of the repressor CggR to its single DNA target sequence is modulated by fructose-1,6-bisphosphate, Mol. Microbiol. 47 (2003) 1709−1721.

[12] M. Fonvielle, M. Coinçon, R. Daher, N. Desbenoit, K. Kosieradzka, N. Barilone, B. Gicquel, J. Sygusch, M. Jackson, M. Therisod, Synthesis and biochemical evaluation of selective inhibitors of Class II fructose bisphosphate aldolases: towards new synthetic antibiotics, Chem. Eur J. 14 (2008) 8521−8529.

[13] E. Ling, G. Feldman, M. Portnoi, R. Dagan, K. Overweg, F. Mulholland, V. Chalifa-Caspi, J. Wells, Y. Mizrachi-Nebenzahl, Glycolytic enzymes associated with the cell surface of *Streptococcus pneumoniae* are antigenic in humans and elicit protective immune responses in the mouse, Clin. Exp. Immunol. 138 (2004) 290−298.

[14] K.M. Kondratyuk, E.I. Lukashuk, A.V. Golovchenko, E.B. Rusanov, V.S. Brovarets, Reaction of diethyl 1-acylamino-2,2-

dichloroethenylphosphonates with amino acids esters, Russ. J. Gen. Chem. 82 (2012) 643−651.

[15] K.M. Kondratyuk, E.I. Lukashuk, A.V. Golovchenko, A.N. Vasilenko, V.S. Brovarets, Synthesis and some properties of 4-phosphorylated derivatives of 5-mercapto-1,3-oxazoles, Russ. J. Gen. Chem. 83 (2013) 46−53.

[16] A. Bauer, W. Kirby, J. Sherris, M. Turck, Antibiotic susceptibility testing by a standardized single disk method, Am. J. Clin. Pathol. 45 (1966) 493−496.

[17] https://www.uniprot.org/uniprot/P9WQA3.

[18] https://www.uniprot.org/uniprot/Q9URB4.

[19] S.F. Altschul, W. Gish, W. Miller, E.W. Myers, D.J. Lipman, Basic local alignment search tool, J. Mol. Biol. 215 (1990) 403−410.

[20] A. Waterhouse, M. Bertoni, S. Bienert, G. Studer, G. Tauriello, R. Gumienny, F.T. Heer, T.A.P. de Beer, C. Rempfer, L. Bordoli, R. Lepore, T. Schwede, SWISS-MODEL: homology modelling of protein structures and complexes, Nucleic Acids Res. 46 (2018) 296−303.

[21] C. Camacho, G. Coulouris, V. Avagyan, N. Ma, J. Papadopoulos, K. Bealer, T.L. Madden, BLAST+: architecture and applications, BMC Bioinf. 10 (2009) 421−430.

[22] M. Remmert, A. Biegert, A. Hauser, J. Soding, HHblits: lightning-fast iterative protein sequence searching by HMM-HMM alignment, Nat. Methods 9 (2012) 173−175.

[23] C. Colovos, T.O. Yeates, Verification of protein structures: patterns of nonbonded atomic interactions, Protein Sci. 2 (1993) 1511−1519.

[24] R.A. Laskowski, M.W. MacArthur, D.S. Moss, J.M. Thornton, PROCHECK - a program to check the stereochemical quality of protein structures, J. App. Cryst. 26 (1993) 283−291.

[25] I. Semenyuta, V. Kovalishyn, V. Tanchuk, S. Pilyo, V. Zyabrev, V. Blagodatnyy, O. Trokhimenko, V. Brovarets, L. Metelytsia, 1,3-Oxazole derivatives as potential anticancer agents: computer modeling and experimental study, Comput. Biol. Chem. 65 (2016) 8−15.

[26] M. Trush, I. Semenyuta, S. Vdovenko, S. Rogalsky, E. Lobko, L. Metelytsia, Synthesis, spectroscopic and molecular docking studies of imidazolium and pyridinium based ionic liquids with HSA as potential antimicrobial agents, J. Mol. Struct. 1137 (2017) 692−699.

[27] M.V. Kachaeva, D.M. Hodyna, I.V. Semenyuta, S.G. Pilyo, V.M. Prokopenko, V.V. Kovalishyn, L.O. Metelytsia, V.S. Brovarets, Design, synthesis and evaluation of novel sulfonamides as potential anticancer agents, Comp. Biol. Chem. 74 (2018) 294−303.

[28] M.F. Sanner, Python: a programming language for software integration and development, J. Mol. Graph. Model. 17 (1999) 57−61.

[29] Dassault Systèmes BIOVIA, Discovery Studio, Dassault Systèmes, San Diego, 2018, 2.5.5.

[30] ChemAxon MarvinSketch, 2018, version 5.3.735. http://www.chemaxon.com.

[31] M.D. Hanwell, D.E. Curtis, D.C. Lonie, T. Vandermeersch, E. Zurek, G.R. Hutchison, Avogadro: an advanced semantic chemical editor, visualization, and analysis platform, J. Cheminf. 4 (2012) 17.

[32] G.M. Morris, R. Huey, W. Lindstrom, M.F. Sanner, R.K. Belew, D.S. Goodsell, A.J. Olson, Autodock4 and AutoDockTools4: automated docking with selective receptor flexiblity, J. Comput. Chem. 16 (2009) 2785−2791.

[33] X. Han, X. Zhu, Z. Hong, L. Wei, Y. Ren, F. Wan, S. Zhu, H. Peng, L. Guo, L. Rao, L. Feng, J. Wan, Structure-based rational design of novel inhibitors against fructose-1,6-bisphosphate aldolase from *Candida albicans*, J. Chem. Inf. Model. 57 (2017) 1426−1438.

[34] G.C. Capodagli, W.G. Sedhom, M. Jackson, K.A. Ahrendt, S.D. Pegan, A noncompetitive inhibitor for Mycobacterium tuberculosis's class IIa fructose 1,6-bisphosphate aldolase, Biochemistry 53 (2014) 202−213.

[35] https://pubchem.ncbi.nlm.nih.gov/bioassay/588726.

[36] https://pubchem.ncbi.nlm.nih.gov/bioassay/651616.

[37] https://pubchem.ncbi.nlm.nih.gov/bioassay/652141.

[38] ChemAxon Instant JChem, 2018, version 5.3.8. http://www.chemaxon.com.

[39] http://www.rcsb.org/structure/4LV4.

[40] S.D. Pegan, K. Rukseree, S.G. Franzblau, A.D. Mesecar, Structural basis for catalysis of a tetrameric class IIa fructose 1,6-bisphosphate aldolase from Mycobacterium tuberculosis, J. Mol. Biol. 386 (2009) 1038−1053.

[41] D.R. Hall, G.A. Leonard, C.D. Reed, C.I. Watt, A. Berry, W.N. Hunter, The crystal structure of Escherichia coli class II fructose-1,6-bisphosphate aldolase

in complex with phosphoglycolohydroxamate reveals details of mechanism and specificity, J. Mol. Biol. 287 (1999) 383−394.

[42] A.J. Wiemer, D.F. Wiemer, Prodrugs of phosphonates and phosphates: crossing the membrane barrier, Top. Curr. Chem. 360 (2015) 115−160.

[43] C.M. Sevrain, M. Berchel, H. Couthon, P.A. Jaffrès, Phosphonic acid: preparation and applications, Beilstein J. Org. Chem. 13 (2017) 2186−2213.

[44] U. Sharma, D. Pal, R. Prasad, Alkaline phosphatase: an overview, Indian J. Clin. Biochem. 29 (2014) 269−278.

[45] P.J. O'Brien, D. Herschlag, Alkaline phosphatase revisited: hydrolysis of alkyl phosphates, Biochemistry 41 (2002) 3207−3225.

[46] M. Yordanov, P. Dimitrova, S. Patkar, L. Saso, N. Ivanovska, Inhibition of Candida albicans extracellular enzyme activity by selected natural substances and their application in Candida infection, Can. J. Microbiol. 54 (2008) 435−440.